Flare Irradiance Spectral Model (FISM) use for space weather applications

Phillip C. Chamberlin[1], Thomas N. Woods[1] , and Francis G. Eparvier[1]

[1] Laboratory for Atmospheric and Space Physics, University of Colorado, 1234 Innovation Dr., Boulder, CO 80303, USA.

Abstract. The solar photon output from the Sun, which was once thought to be constant, varies considerably over time scales from seconds during solar flares to years due to the solar cycle. This is especially true in the wavelengths shorter than 190 nm. These variations cause significant deviations in the Earth and space environment on similar time scales, which then affects many things including satellite drag, radio communications, atmospheric densities and composition of particular atoms, molecules, and ions of Earth and other planets, as well as the accuracy in the Global Positioning System (GPS). The Flare Irradiance Spectral Model (FISM) is an empirical model that estimates the solar irradiance at wavelengths from 0.1 to 190 nm at 1 nm resolution with a time cadence of 60 seconds. This is a high enough temporal resolution to model variations due to solar flares, for which few accurate measurements at these wavelengths exist, as well as the solar cycle and solar rotation variations. The FISM algorithms are given, and results and comparisons are shown that demonstrates the FISM estimations agree within the stated uncertainties to the various measurements of the solar VUV irradiance.

Index Terms. solar variations, solar irradiance, space weather, ultraviolet.

1. Introduction

Measurements of solar VUV irradiance represent a valuable data set, with historically extensive suites, as well as several current and planned observational platforms. Despite these numerous measurements, there are still frequent and long-duration data gaps, most notably including the pre-instrumental period (prior to 1946), the period from 1980 to 1998 for the EUV range, and shorter time gaps of minutes to hours that routinely occur between satellite instrument observations.

Four of the most widely used solar VUV irradiance models to fill these gaps are the HFG model (Hinteregger *et al.*, 1981), the EUVAC model (Richards *et al.*, 2005), the SOLAR2000 model (Tobiska, 2004), and the NRLEUV model (Warren *et al.,*2001). All of these models, except NRLEUV, were initially based on Atmospheric Explorer-E (AE-E) data and several sounding rocket flights. The SOLAR2000 model has been updated to include TIMED SEE data as a reference data set in the VUV range.

A comparison of the output from these four models to the data from Thermosphere Ionosphere Mesosphere Energetics and Dynamics (TIMED) Solar Extreme ultraviolet Experiment (SEE) (Woods *et al.*, 1998) was given in Woods *et al.* (2005). This paper shows the large differences, with SEE being about 70% higher than the EUV81 and NRLEUV values in the 5-25 nm broadband range, and EUV81 about 50% higher in the 50-75 nm range than the SEE over the duration of the SEE mission at the time of the publications (Feb 2002-Mid 2004). This shows that significant improvements in the models are needed in order to accurately reproduce the solar irradiance for a given day.

2. Improvements of FISM over Previous Models

The advantage of FISM over other models is that FISM allows a more accurate determination of the solar XUV, EUV, and FUV irradiances. The FISM algorithms and data sets used resolve most of the discrepancies between the other models and the SEE data, including the large solar cycle offsets and temporal discrepancies due to large active regions.

A significant improvement for FISM over other empirical models is its use of recent, more accurate measurements of the EUV irradiance from the SEE instrument onboard the TIMED satellite, the FUV irradiance measurements from SEE as well as from Upper Atmosphere Research Satellite (UARS) SOLar Stellar Irradiance Comparison Experiment (SOLSTICE) (Rottman *et al.*, 1993), and also the XUV and short-wavelengths EUV measurements from both the SEE and SORCE versions of XPS. Along with SEE making approximately 11 observations a day to compute a daily average, the SEE measurements include observations of over 40 flares of GOES M class or higher. Acquiring these data sets is statistically crucial in making good fits with the proxies. Along with SEE providing a statistically significant improvement in the number of VUV irradiance measurements, it also has a much smaller uncertainty due to the calibration method than previous satellites that have measured the EUV. This calibration method was discussed in more detail in Chamberlin *et al.* (2005). With the much smaller uncertainties of the SEE and SOLSTICE data, a model based on these data, as FISM is, will be much more accurate than other models based on the measurements from

AE-E.

Another significant improvement of FISM is that it can model the solar irradiance with up to a 3-second temporal resolution, although the standard output is currently at 60-seconds, while other models only give one averaged value for a day. The previously discussed daily models neglect some of the very rapid, large-magnitude changes in the XUV, EUV and FUV irradiance due to large solar flares that can have a significant impact on Earth, and can underestimate the integrated daily averaged solar irradiance from 0.1-120.0 nm by more than 13% for a day containing a single X-class flare. The higher temporal scale for FISM will allow atmospheric models to calculate the effects of the changing solar irradiance on Earth more accurately on shorter time intervals.

FISM also makes use of different proxies that have not currently been utilized in current models, which will be discussed in further detail in Section 3. These include the 0-4 nm band, the 1-nm bin centered at 36.5 nm, and the 1-nm bin centered at 30.5 nm. These emissions are used as proxies in order to more accurately model the solar rotation temporal irradiance changes of their similar emission processes and temperatures by providing a more accurate center-to-limb response.

3. Proxies

Six different proxies are used, when available, to represent the solar cycle and solar rotation daily irradiance variations and provide the most accurate estimation of the solar VUV irradiance for a particular day. These six proxies have different formation temperatures; therefore, these proxies are formed in different layers of the solar atmosphere, and most accurately represent those emissions with a similar formation temperature. The GOES 0.1-0.8 nm channel, along with the time derivative of this irradiance measurement are used as a proxy to represent the variations due to flares.

3.1. Daily Component Proxies

The 10.7 cm radio flux, or F10.7, represents the coronal continuum (Bremsstrahlung) emissions, and has a long history of calibrated measurements as far back as 1947. A more representative proxy for this type of emission is the XUV irradiance itself, which the 0-4 nm integrated irradiance from TIMED SEE will be used, when available. The proxy used for the coronal VUV emissions with have a strong center-to-limb brightening affect is the 1 nm bin centered on 36.5nm from the SEE measurements. This bin contains various coronal emissions, including the Fe XVI emission (36.076 nm) formed at 2.5MK along with a Mg IX emission (36.8 nm) which has a formation temperature which is slightly lower in the corona at 1MK. Another proxy that was studied due to it being a very dominant emission in the EUV range is the He II 30.4 nm (25,000 K) emission line, which is used as a proxy for the upper transition region emissions. Another proxy used for the transition region is the neutral hydrogen Lyman-α emission line at 121.6 nm, hereafter referred to as Lyα. The Mg II core-to-wing ratio (Heath and Schlesinger, 1986) most accurately portrays the chromospheric emissions, along with the continuum emissions in the FUV wavelengths.

3.2. Flare Proxies

The long wavelength channel on the GOES X-ray sensor (XRS) provides a value of the 0.1 to 0.8 nm irradiance. The GOES XRS was specifically designed to monitor these highly variable wavelengths that increase by orders of magnitude during large flares, while it also has the sensitivity range to capture many small flares. Because GOES XRS values are currently the only near real-time data that are given on time scales short enough to represent various changes in irradiance due to flares, the GOES 0.1-0.8 nm fluxes are used as the short-term, solar flare proxy for FISM.

There is question as to whether or not the coronal soft X-rays measured by the GOES XRS can accurately represent the EUV and FUV irradiance changes during a solar flare, as these emissions are formed in different regions of the flare structure. The soft X-ray fluxes have been shown to correlate with the main-phase EUV irradiance changes from a flare (Priest, 1981). This relationship has been shown for both the time duration of the flare and also shows simultaneous peak times, but these results may also be due to inaccuracies or limitations of the observations, and may only represent one specific type of flare. It was also initially derived by Neupert (1968) that the positive time derivative of the soft X-ray irradiance is an accurate temporal representation of the hard X-ray, impulsive phase of the flare. This relationship is now referred to as the 'Neupert effect', and is important for FISM as the impulsive hard X-rays are shown to correlate with the impulsive phase of EUV measurements, both temporally and energetically (McClymont and Canfield, 1986; and others).

4. FISM Concept

The FISM concept to model the solar irradiance is that the irradiance for a particular wavelength λ at time t, $E(\lambda,t)$, has solar variations above a constant minimum irradiance value, $E_{min}(\lambda)$. Additional components added to the minimum irradiance value are the variations due to solar cycle, ΔE_{SC}, solar rotation of active regions, ΔE_{SR}, and also the impulsive and gradual phases of solar flares, ΔE_{IP} and ΔE_{GP}. This relationship is given as:

$$E(\lambda,t) = E_{\min}(\lambda) + \Delta E_{SC}(\lambda,t) + \Delta E_{SR}(\lambda,t) + \Delta E_{GP}(\lambda,t) + \Delta E_{IP}(\lambda,t). \quad (1)$$

FISM models the solar cycle and solar rotation irradiance changes as a relative change above a constant minimum value based on the proxies' relative change above its minimum value. The flare components, both the impulsive and gradual phase, are modeled as absolute values above the daily value, which includes the solar cycle minimum value plus the irradiance contributions from both solar cycle and solar rotation components. Each type of irradiance variation is modeled separately, and the form and algorithms for each of the individual ΔE components in Eq. 1 are discussed in the following sections.

5. FISM Algorithms

5.1. FISM Solar Cycle Algorithms

The long-term variations above the minimum reference value are the first to be modeled by FISM, and these variations are dominated by the 11-year solar cycle variations. The relative change over the solar cycle is modeled by the linear equation:

$$\left[< E_d(\lambda,t_d) >_{108} - E_{\min}(\lambda)\right] / E_{\min}(\lambda) = C_0(\lambda) + C_{SC}(\lambda)\left[< P_d(t_d) >_{108} - P_{\min}\right] / P_{\min}, \quad (2)$$

where

$$< E_d(\lambda,t_d) >_{108} - E_{\min}(\lambda) = \Delta E_{SC}(\lambda,t_d). \quad (3)$$

The 108-day average for the proxy, $<P_d(t_d)>_{108}$, is the 108-day mean value centered at day d, and the formulation is similar to find the 108-day average for the irradiance measurements, $<E_d(\lambda,t_d)>_{108}$. The coefficients $C_0(\lambda)$ and $C_{SC}(\lambda)$ give the linear relationship between the relative change of the solar cycle proxy value to the relative change of the solar cycle irradiance value for each wavelength. A linear fit is performed to solve for $C_0(\lambda)$ and $C_{SC}(\lambda)$ using the SEE daily average values (Level 3) for the XUV and EUV wavelengths and the UARS SOLSTICE (from 1992 until 1996) for the FUV at all available times, t, for $E_d(\lambda,t_d)$, and then the corresponding proxy values for these times as $P_d(t_d)$.

5.2. FISM Solar Rotation Algorithms

The absolute changes in the irradiance due to the solar rotation are given by subtracting the 108-day solar cycle average from the daily average value. Dividing this residual by the minimum reference value then gives the relative change of the solar rotation variations above the solar cycle values. A linear relationship is then fit in order to model the relative change of the solar rotation irradiance to the similarly formed proxy value, or:

$$\left[E_d(\lambda,t_d) - < E_d(\lambda,t_d) >_{108}\right] / E_{\min} = C_1(\lambda) + C_{SR}(\lambda)\left[P_d(t_d) - < P_d(t_d) >_{108}\right] / P_{\min} \quad (4)$$

and

$$E_d(\lambda,t_d) - < E_d(\lambda,t_d) >_{108} = \Delta E_{SR}(\lambda,t). \quad (5)$$

Using the proxies, the relative irradiance change for wavelength bin λ and day t_d can then be found by solving the Eqs. 2 and 4 using the known coefficients. This gives the daily averaged model component of FISM, $E_d(\lambda,t_d)$.

5.3. FISM Gradual Phase Algorithms

As the flare component is the difference between the irradiance and its daily value, for the measurements as well as the proxy, a power law relation was considered due to the large order of magnitude changes that occur in GOES XRS irradiances. The gradual phase flare algorithm is:

$$E(\lambda,t_{UTC}) - E_d(\lambda,t_d) = C_{GP}(\lambda)\left[P(t_{UTC}) - P_d(t_d)\right]^{N_{GP}(\lambda)} \quad (6)$$

where

$$E(\lambda,t_{UTC}) - E_d(\lambda,t_d) = \Delta E_{GP}(\lambda,t_{UTC}). \quad (7)$$

$N_{GP}(\lambda)$ equals 1 for the soft X-rays (λ < 14 nm), and therefore Eq. 6 is then just a linear equation, while the $N_{GP}(\lambda)$ average for the EUV wavelengths (λ > 14 nm) is 0.647. $P_d(t_d)$ and $E_d(\lambda,t_d)$ are the daily averaged proxy and irradiance value measurements for the day t_d, just as they were in all previous equations in this chapter. $P(t_{utc})$ and $E(\lambda,t_{utc})$ are then the proxy and irradiance values during a specific time, t_{UTC}, during the day, t_d, in UTC seconds of the day.

5.4. FISM Impulsive Phase Algorithms

Given the relationship of the Neupert effect (Neupert, 1968), which states the time derivative of the gradual phase of the flare gives the temporal profile of the impulsive phase of the flare, the FISM impulsive phase algorithm is

$$\left[E(\lambda,t_{UTC}) - E_d(\lambda,t_d)\right] = f(\mu,\lambda) \bullet C_{IP}(\lambda)\left[\frac{d}{dt}\left(P(t_{UTC}) - P_d(t_d)\right) > 5x10^{-10}\right]^{N_{IP}(\lambda)} \quad (8)$$

where

$$E(\lambda,t_{UTC}) - E_d(\lambda,t_d) = \Delta E_{IP}(\lambda,t_{UTC}). \quad (9)$$

The irradiance and proxy values are once again given as the measured values at time t_{UTC} and the daily values for day t_d, as they were for Eq. 6. The CLV correction, $f(\mu,\lambda)$, is derived from the gradual phase CLV of observed flares. The derivative of the GOES proxy irradiance is limited to be greater than $5x10^{-10}$ in order to have variations only during the rise of the gradual phase and to eliminate minor fluctuations of the derivative that are due to measurement noise and not actual solar variability.

5.5. FISM Uncertainty

The FISM daily component uncertainty is found by determining the weighted standard deviation of the FISM daily results from the SEE Level 3 data for the almost 4 years of available SEE data using the equation given by Bevington's (1969) analysis of a least-squared fit to a line, or:

$$\sigma(\lambda) = \sqrt{\frac{\sum_{i=0}^{n}\left[\frac{E_P(i) - E_{Meas}(i,\lambda)}{E_{Meas}(i,\lambda)}\right]^2}{n-2}}. \quad (10)$$

A linear fit contains two degrees of freedom, which is why n-2 is used in the denominator. This is done for the time series of each proxy, E_P, and for each wavelength, E_{Meas},when both components are available. The FISM 'total uncertainty' is the FISM uncertainties added in quadrature with the uncertainties of the base data set.

6. FISM Results and Comparisons

The 1-nm bins of FISM are combined in order to make a similar broadband data product as the SEM products. Fig. 1 shows the FISM and the Solar EUV Monitor (SEM, Judge *et al.* 1998) daily averaged results for the 26-34 nm channels during solar cycle 23. There are many spikes in the SEM data, caused by large increases in the counts due to its sensitivity to high-energy particles, which are not yet removed from the SEM data. Nonetheless, SEM provides a data set for which to make comparisons of the FISM results for almost one complete solar cycle.

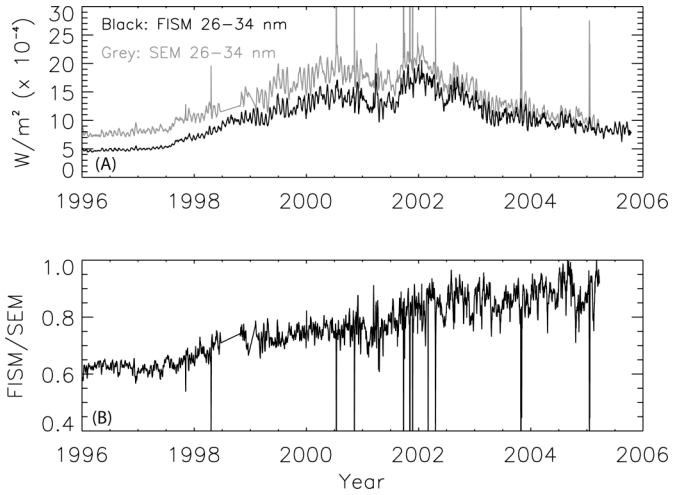

Fig. 1. (A) Time series of the FISM integrated results from 26-34 nm and the SEM 26-34 nm channel over the time of the SEM mission. (B) The ratio of the FISM estimates to the SEM measurements.

There is an approximately 10% offset in the FISM and SEM data for the optimal time period from 2002 until present, which is also present when comparing the SEE data for which FISM was derived from to the SEM data. The differences between the SEM data and FISM results increase before 2002 due to the loss of the 30.5 nm, 36.5 nm, and 0-4 nm optimal proxies, for which the Lyα and F10.7 proxies are then used in their place. The discrepancies between the FISM and SEM data during solar minimum conditions may also be due to errors in extrapolating the existing SEE data to determine the FISM solar minimum reference spectrum**.** The solar minimum results from FISM are expected to improve in the next two years as TIMED SEE, SOHO SEM, and SORCE SOLSTICE all will measure the solar VUV irradiance during the upcoming solar minimum.

The Results of the 28 October 2003 flare from FISM are also compared to the SEM 26-34 nm data at 15-second temporal resolution in Fig. 2. As stated previously, the SEE data is approximately 10% lower then the SEM data, and this offset is transferred to the FISM data; therefore the SEM data in Fig. 2 are multiplied by a factor of 0.9 to account for this difference. The absolute values between FISM and SEM results show very good agreement when this discrepancy between the two data sets is considered. The large increase in the SEM data seen in Fig. 2, starting around 12:15 UTC, is due to high-energy particles associated with this X17.2 flare.

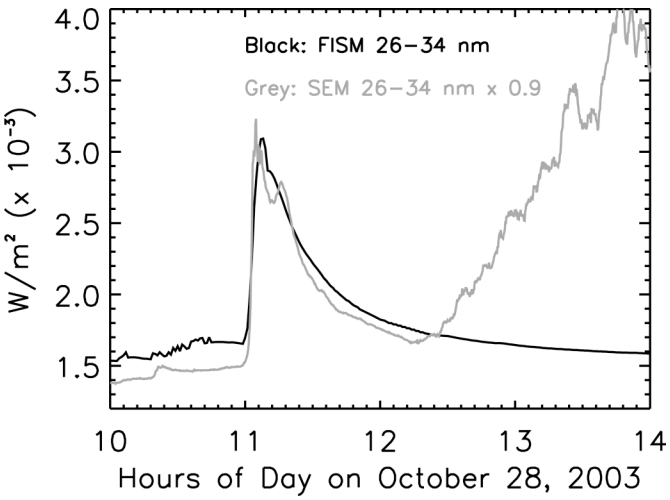

Fig. 2. The FISM 26-34 nm estimates (Black, 60 sec temporal resolution) and the similar SEM measurements (Grey, 15 sec temporal resolution) during the X17 flare that occurred on 28 October 2003.

7. Conclusion

FISM has been shown to accurately estimate the solar irradiance taking into account the changes due to solar cycle, solar rotation, and flares. FISM data may be requested by contacting the author at phil.chamberlin@lasp.colorado.edu.

Acknowledgments. This work was supported by NASA grant NAG5-11408 at the University of Colorado.

References

Bevington, P. R., *Data Reduction and Error Analysis for the Physical Sciences*, McGraw-Hill, New York, 1969.

Chamberlin, P. C., T. N. Woods, and F. G. Eparvier, Rocket Extreme ultraviolet Grating Spectrometer (EGS): calibrations and results of the solar irradiance on February 8, 2002, *Proc. SPIE Int. Soc. Opt. Eng.,* vol. 5538, pp. 31-42, 2004.

Heath, D. F., and B. M. Schlesinger, The Mg 280-nm doublet as a monitor of changes in solar ultraviolet irradiance, *J. Geophys. Res.*, vol. 91, pp. 8672-8682, 1986.

Hinteregger, H. E., K. Fukui, and B. R. Gilson, Observational, reference, and model data on solar EUV, from measurements on AE-E, *Geophys. Res. Lett.*, vol. 8, 1147-1150, 1981.

Judge, D. L., *et al.*, First solar EUV irradiances obtained from SOHO by the CELIAS/SEM, *Solar Phys.*, vol. 177, pp. 161-173, 1998.

McClymont, A. N., and R. C. Canfield, The solar flare extreme ultraviolet to hard X-ray ratio, *Astrophys. J.,* vol. 305, pp. 936-946, 1986.

Neupert, W. N., Comparison of solar X-ray line emission with microwave emission during flares, *Astrophys. J.,* vol. 153, p. L59, 1968.

Priest, E. R., in *Solar Flare Magnetohydrodynamics*, E. R. Priest (ed.), Gordon and Breach Science Publishers, New York, 1981.

Richards, P. G., T. N. Woods, and W. K. Peterson, HEUVAC: a new high resolution solar EUV proxy model, *Adv. Space Res.*, in press, 2005.

Rottman, G. J., T. N. Woods, and T. P. Sparn, SOLar Stellar Irradiance Comparison Experiment I: 1. Instrument design and operation, *J. Geophys. Res.,* vol 98*,* pp. 10,667-10,677, 1993.

Tobiska, W. K., SOLAR2000 irradiances for climate change research, aeronomy, and space system engineering, *Adv. Space Res.*, vol. 34, pp. 1736-1746, 2004.

Warren, H. P., J. T. Mariska, and J. Lean, A new model of solar EUV irradiance variability 1. Model formulation, *J. Geophys. Res.*, vol. 106, pp. 15,745-15,757, 2001.

Woods, T. N., *et al.*, TIMED solar EUV experiment, *SPIE*, vol. 3442, pp. 180-191, 1998.

Woods, T. N., *et al.*, Solar EUV Experiment (SEE): Mission overview and first results, *J. Geophys. Res.*, vol. 110, A01312, 2005, doi:10.1029/2004JA010765.